Journal of Information Hiding and Multimedia Signal Processing ©2025 ISSN 2073-4212
Ubiquitous International Volume **16**, Number **3**, September **2025**

Enhanced Brain Tumor Classification Using Optimized U-Net Segmentation by EPO and Hybrid Feature Extraction Using FO

Kondra Pranitha

Research Scholar, Department of CSE
Koneru Lakshmaiah Education Foundation
Vaddeswaram, AP, India
kondra.pranitha@gmail.com

Vuda Sreenivasa Rao*

Associate Professor, Department of CSE
Koneru Lakshmaiah Education Foundation
Vaddeswaram, AP, India
vsreenivasarao@kluniversity.in

*Corresponding author: Vuda Sreenivasa Rao
Received March 14, 2025, revised June 26, 2025, accepted July 9, 2025.

Abstract. *The accurate classification of brain tumors plays a pivotal role in the timely and effective treatment of patients. In this study, we propose a novel approach to enhance brain tumor classification by incorporating advanced feature extraction techniques with enhanced segmentation algorithms. The developed framework incorporates an improved U-Net architecture for precise tumor segmentation and a hybrid transfer learning algorithm for effective feature extraction. The proposed methodology commences with the collection of BraTS 2020 available publicly and pre-processing of brain tumor images. This pre-processing phase enhances the quality of images by reducing noise and irrelevant background content. After this step, a tumor region growing U-Net algorithm is applied so that the growing region of the tumor is accurately represented and bound. Such images are segmented and processed further in the feature extraction module. A hybrid feature extractor that combines Firefly Optimization (FO) metaheuristic with ResNet-50-based transfer learning is proposed. This unique approach captures and exploits the most salient features that can be found within the data. They are extracted and put through a deep convolutional neural network designed to classify all trained types of tumors, thus achieving a high accuracy rate. Weight and bias refinement within the U-Net architecture is done through the Emperor Penguin Optimizer (EPO), which aims to reduce the cross-entropy loss. The designed framework works with a given Python tool, and its performance is analyzed based on standard measures: correctness, precision, and F1 measurement. The results reported for these measures are 99.80%, 99.44%, and 99.55%, which demonstrate the effectiveness of the approach.*

Keywords: brain tumor; deep convolutional neural network; feature extraction; segmentation; transfer learning

1. **Introduction.** The brain is a complex organ of the human body that regulates the entire nervous system. It contains millions of nerve cells that are responsible for controlling and regulating body functions [1]. Hence, any abnormality in this organ puts

human health in danger. Brain tumor (BT) is an abnormality, that indicates uncontrolled proliferation of cells in the brain tissue [2]. Brain tumors are typically categorized into two classes, namely benign and malignant. The benign are non-cancerous, while the malignant are cancerous. The malignant class is further classified into three subtypes: meningioma, glioma, and pituitary [3]. The World Health Organization (WHO) study reported that meningioma, glioma, and pituitary prevalence rates are 45%, 15%, and 15%, respectively [4]. The accurate detection and classification of these tumors is essential for proper treatment planning and safeguarding the person from death.

However, the identification and categorization is complex because of its intricate characteristics like location, size, etc., [5]. Various imaging tools, including ultrascopy, computed tomography (CT), magnetic resonance imaging (MRI), etc., have been developed to assist in tumor classification [6]. MRI images are widely used in clinical studies to analyze brain anatomy. The MRI technique offers improved image resolution and contrast, assisting healthcare professionals in precisely detecting specific diseases [7]. The conventional methods of tumor detection involve manually analyzing the MRI images, which is time-consuming and needs more experienced personnel. Moreover, manual detection is prone to errors, making it less reliable and ineffective [8]. These drawbacks in manual detection demand an automatic classification model for brain tumor prediction.

Hence, computer-aided diagnostic techniques are developed for automatically detecting and classifying brain tumors [9]. Accurate categorizations assist doctors in treating patients. Many studies are done on automatic brain tumor classification, which uses advanced image processing algorithms like machine learning and deep learning [10]. These models deploy supervised or unsupervised learning techniques to understand healthy and pathological tissue differences. Although these models are more effective than manual detection, accurate segmentation of tumor regions is still the biggest concern [11, 12]. Separating pathological and healthy brain tissues is significant in tumor treatment plans and cancer research. This accurate segmentation helps doctors treat tumors precisely, improving their survival rates [13]. Image segmentation remains an important task in medical image analysis, which involves discarding the regions of interest (ROI) from images [14]. Typically, this process is too long and imposes several challenges while processing large databases. The traditional way of image segmentation includes thresholding, in which certain threshold values are set to fragment the normal and abnormal tissues from the MRI images [15, 16]. This methodology creates obstacles to the automatic diagnosis of tumors, demanding a precise automatic image segmentation algorithm for proper detection and treatment [17]. The accurate segmentation of tumor regions is significant for improving the classification process.

In addition to this, the existing works face difficulty in feature analysis. Effective feature extraction is vital in distinguishing healthy and pathological tissues [18, 19, 20]. Practical feature engineering significantly improves model training and reduces computational time. Few existing studies utilized techniques such as a Support Vector Machine with a pre-trained DL algorithm [21], Generative Adversarial Network [22], Convolutional Neural Network [23], DeepTumorNet [24], etc., for automatic segmentation and classification of brain tumors. In order to improve diagnostic accuracy and extract useful information from medical images, this study investigates a variety of machine learning and deep learning techniques, including fuzzy C-means, KNN, SVM, decision trees, G-CNN, ANN, CRF-RNN, DNN, and Naive Bayes classifiers. It gives practitioners and researchers new perspectives [26]. Amudha's [40] proposed brain tumor detection framework uses a Multiscale Frangi Gaussian Matrix and a stacked CNN architecture for MRI analysis, enhancing vessel structure enhancement and tumor classification. It incorporates Frangi

filters, spatial channel-wise attention, CatBoost, and Extremely Randomized Trees. Despite higher classification accuracy, these models face challenges like higher computational resources, large time consumption, limited scalability, lower generalization, etc. To resolve these issues, we presented an improved segmentation and feature extraction algorithm for improved tumor classification.

The major contributions of the study are described below,

- This study aims to create an enhanced image segmentation algorithm using the improved deep learning model to separate the tumor and healthy tissues accurately.
- A hybrid feature extraction model was developed, combining the efficiencies of deep learning and meta-heuristic optimization techniques to effectively capture and extract the most essential and relevant features.
- This study employs the deep convolutional neural network architecture as the classification model, which was trained using the extracted features to differentiate the benign and malignant tumors.
- The developed algorithm was designed using the Python tool, and the results are evaluated and validated with conventional techniques in terms of accuracy, precision, recall, and f-measure.

2. **Related Works.** A few research works associated with the brain tumor classification are reviewed below,

Muhammad Imran Sharif et al. [21] developed an automatic approach for categorizing multiclass brain tumors. This study utilized the pre-trained DL algorithm to balance the data in the training phase. Also, Entropy-Kurtosis-based High Feature Values and a Modified Genetic Algorithm were deployed to extract and select the most significant features from the MRI images. Finally, a Support Vector Machine (SVM) classification model was employed for multiclass tumor categorization. This work was experimented with the two publicly available databases, BRATS2018 and BRATS2019. The implementation outcomes offered high accuracy of 95.15% and 95.74% in tumor classification. However, this technique faces challenges in offering generalization to unseen samples.

Navid Ghassemi et al. [22] developed a deep-learning approach for classifying tumors using MRI images. In this study, a DNN was first pre-trained as a differentiator in a generative adversarial network on various databases to capture unique and distinct attributes. This process enables the system to learn the structure of a tumor effectively. This study was validated using the MRI dataset containing 3064 T1-CE images collected from 233 patients. The experimental results show that this algorithm obtained 95.47% accuracy in classifying the three tumor instances (meningioma, glioma, and pituitary). However, the computational complexity of the system is high.

Muhammad Aamir et al. [23] designed an effective automatic brain tumor diagnosis using MRI images. The primary concern of this work is to resolve the challenges associated with manual tumor detection. Here, the brain MRI images are gathered and filtered to improve visual quality. Consequently, two different pre-trained DL models capture the most significant attributes. Finally, a convolutional neural network (CNN) was utilized to categorize benign and malignant tumors. This collaborative mechanism achieved a higher accuracy of 98.95% and minimal computational time. However, fine-tuning CNN architecture is complex and consumes more computational resources.

Kuraparthi et al. [25] developed a classification model to detect brain tumor cases accurately using MRI images. This study executed three pre-trained DCNN models, AlexNet, ResNet50, and VGG16, as the transfer learning models to capture and extract the most significant attributes from the images. These extracted feature vectors were fed into the SVM classifier for training to categorize the tumor cases. This algorithm

was validated using the Kaggle and BraTs databases and attained 98.86% and 98.24% accuracy. However, this method is prone to overfitting, which limits its generalization ability to real-time scenarios. Table 1 presents the literature survey.

Qureshi et al. [38] proposed a deep learning framework called RobU-Net, a modified U-Net architecture, for robust segmentation of brain tumors in MRI images. Their method is specifically designed to handle Rician noise using discrete wavelet transforms for contrast enhancement and various encoder-decoder structures for improved accuracy. Tested on an MRI brain tumor dataset with 3,064 slices, the framework achieved high sensitivity, dice coefficient, and Jaccard index values (up to 0.9831, 0.9781, and 0.9571), outperforming existing methods and demonstrating its effectiveness for noise-impregnated and original MRI scans.

Qureshi et al. [39] proposed a novel two-stage MGMT Promoter Methylation Prediction (MGMT-PMP) system for radiogenomic classification of glioblastoma using multi-omics fused feature space from mpMRI scans. Their framework combines a fine-tuned Deep Learning Radiomic Feature Extraction (DLRFE) module with radiomic features (GLCM, HOG, LBP) and employs a rejection algorithm to refine training data. Using the BraTS-2021 dataset and k-NN and SVM classifiers, the system achieved high accuracy, sensitivity, and specificity (up to 96.84%, 96.08%, and 97.44%), demonstrating its effectiveness for non-invasive prediction of MGMT promoter methylation status to support personalized treatment planning.

Mohammad Anwar Assaad et al. [41] proposed a hybrid method for brain tumor detection in MRI images, combining deep learning and machine learning techniques. CNNs were used to extract features, which were then reduced using an MLP trained with a novel batch-splitting approach. Classification was performed using Euclidean distance and backpropagation, followed by final classification with the KNN algorithm. Their model achieved 97% accuracy, outperforming a standalone CNN model, which achieved 90%, highlighting the effectiveness of a hybrid architecture in medical image analysis.

3. **System Model and Problem Statement.**

Brain tumors are one of the deadly and life-threatening diseases that account for thousands of deaths every year around the world. Hence, the timely and accurate identification of brain tumors is significant for treatment planning and monitoring disease progression. The manual way of brain tumor detection is done by radiologists, which is time-consuming and prone to errors [27]. These issues in manual diagnosis create a demand for an automatic brain tumor classification model. The deep learning models offer a promising solution for automatically identifying and classifying brain tumors using scanned images. In particular, the ResNet-18 architecture is an efficient method that eliminates the need to start from scratch when training a deep convolutional neural network, providing a simple and quick method for disease prediction [28]. The system model of brain tumor classification using the DL model is presented in Figure 1.

The system model includes modules like data collection, data pre-processing, data sampling, classification model, and model evaluation. Many MRI images are collected from patients, containing both benign and malignant images in the data collection module. In the pre-processing module, the images are filtered to enhance their quality, making them reliable and suitable for subsequent analysis. The pre-processed database was split into two sets (training and testing) in data sampling. The training set was used to train the classification model to differentiate the patterns and correlations between normal and malignant tumors. Finally, the testing sequence was used to evaluate the model's performance. Although the DL models offer greater efficiency and accuracy in tumor prediction and classification, they have inherent challenges. Firstly, training the DL models

Table 1. Literature Survey

Authors	Techniques	Results	Merits	Demerits
Muhammad Imran Sharif et al. [21]	Support Vector Machine with pre-trained DL algorithm	Achieved accuracy of 95.15%, and 95.74% for BRATS2018, and BRATS2019	High classification accuracy and effective feature analysis	Limited generalization to unseen samples
Navid Ghassemi et al. [22]	Deep Neural Network Generative Adversarial Network	Achieved accuracy of 95.14%	Improved feature discrimination and tumor classification	High computational complexity
Muhammad Aamir et al. [23]	DL classification model named Convolutional Neural Network	Obtained 98.95% accuracy in tumor detection and classification	Improved accuracy and minimal computational time	Fine-tuning is complex and requires more computational resources
Asaf Raza et al. [24]	DeepTumorNet (Basic Convolutional Neural Network)	High accuracy of 98.56%	Greater accuracy, simple and computationally effective	Limited scalability and less adaptable
Kuraparthi et al. [25]	Support Vector Machine and pre-trained DL models like AlexNet, ResNet50, and VGG16	Acquired accuracies of 98.86% and 98.24%	Fast and improved training and accurate classification of tumor	Overfitting and less generalization
Qureshi et al. [38]	RobU-Net	Sensitivity 0.9831, dice coefficient 0.9781, and Jaccard index 0.9571 values	Effectiveness for noise-impregnated	Limited scalability and less adaptable
Qureshi et al. [39]	A novel two-stage MGMT Promoter Methylation Prediction (MGMT-PMP) system	Achieved high accuracy 96.84%	High accuracy	Limited generalization
Mohammad Anwar Assaad et al. [41]	CNN for feature extraction with KNN Classification	Achieved accuracy of 97%	Efficient feature analysis and high classification accuracy	High computational complexity

requires large databases, making them computationally expensive. Secondly, refining and optimizing the hyper-parameters of the DL model is complex and requires expertise.

Furthermore, the existing DL techniques often get over-trained on the training sequence and cause overfitting, which limits generalization over real-time scenarios. Also, training these models consumes more time, making them less reliable for clinical settings. In addition, image segmentation and feature extraction algorithms are needed to reduce the computational complexity of the classification model for effective and accurate brain

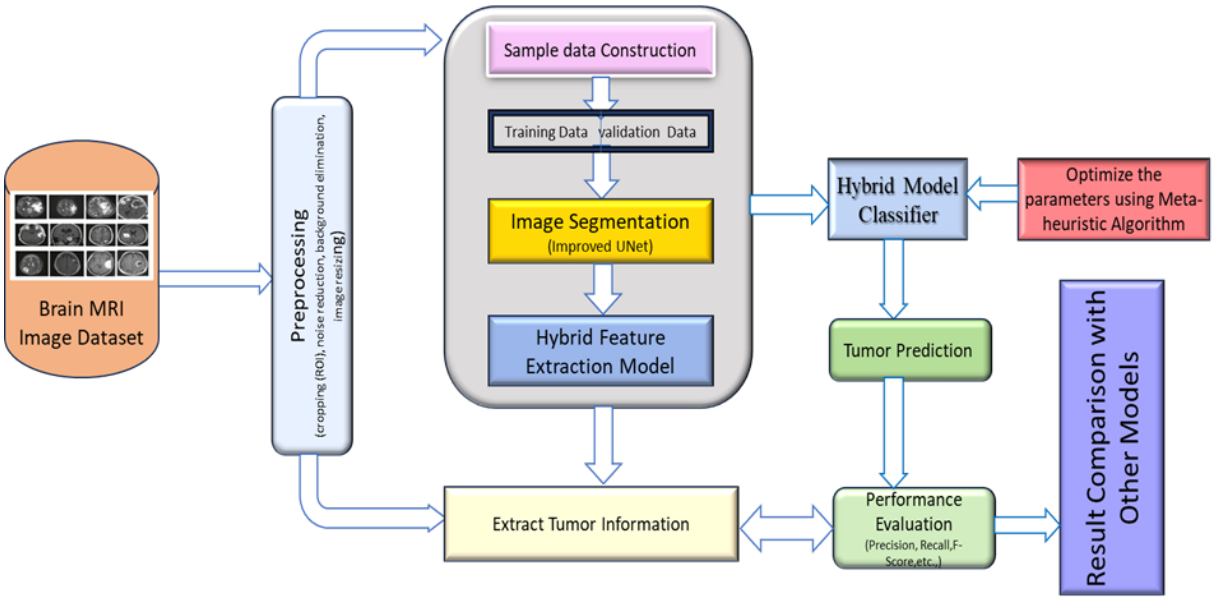

FIGURE 1. Proposed System Architecture

classification. This study worked on providing an optimal solution to all these problems by developing improved segmentation and feature extraction algorithms, which enhance the classifier performance by analyzing the features differentiating the tumor and healthy regions.

4. **Improved Segmentation Using EPO and Feature Extraction by FO.** This study works on developing an improved image segmentation and optimal feature extraction algorithm for accurate brain tumor classification. The proposed work includes five modules: data collection, image preprocessing, segmentation, feature extraction, and classification. Firstly, the brain MRI images are collected and imported into the system in the data collection module. Secondly, the gathered images are preprocessed to improve their quality. In the third module, we developed an image segmentation module using the improved U-Net algorithm with EPO to segment the tumor regions accurately. Following tumor segmentation, feature engineering was performed using the hybrid feature extraction algorithm. In the feature extraction module, we integrate firefly optimization and transfer learning to extract the most discriminative attributes for differentiating health and pathological tissues. Finally, a classification model was developed using the deep convolutional neural network to detect benign and malignant tumors. Here, DCNN was trained using these features to categorize the health and tumors precisely. Figure 2 depicts the architecture of the proposed model.

4.1. **Data collection.** The proposed work involves collecting brain MRI images from patients and healthy individuals in a clinical setting. This dataset contains both MRI scans of normal and tumor patients. In this study, we utilized the publicly available BraTs 2020 database, accessible at `https://www.med.upenn.edu/cbica/brats2020/data.html`. This database contains multi-institutional routine clinically obtained preoperative multimodal 3D MRI scans. It includes scans of glioblastoma (GBM/HGG) and lower-grade glioma (LGG), with pathologically confirmed diagnosis and available overall survival (OS) data. The dataset consists of native (T1), post-contrast T1-weighted (T1Gd), T2-weighted (T2), and T2 Fluid Attenuated Inversion Recovery (T2-FLAIR) volumes. Each scan is segmented manually by one to four raters into different tumor sub-regions, including the

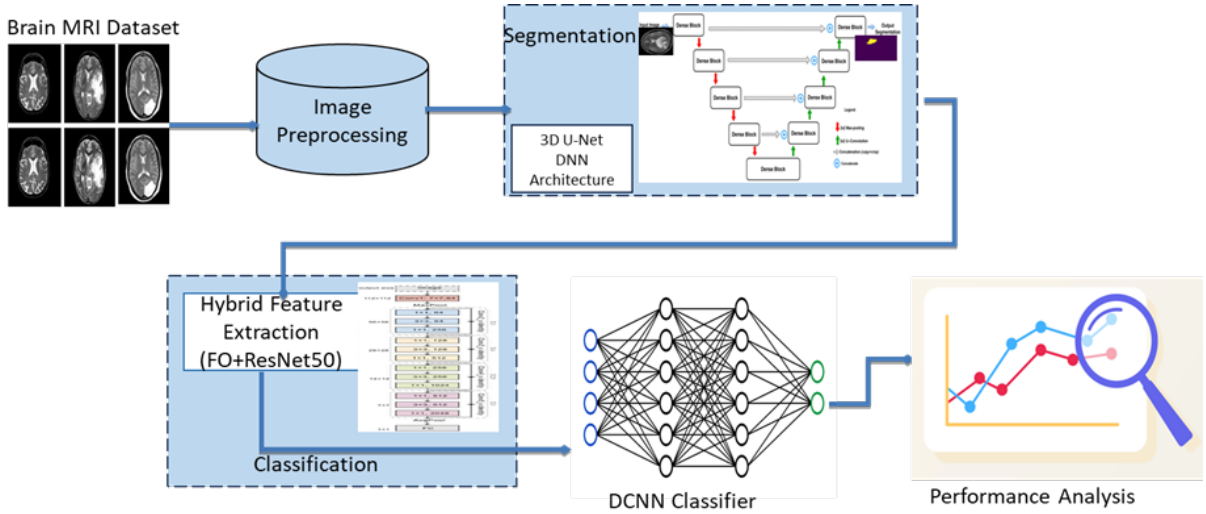

FIGURE 2. Proposed U-Net with EPO and FO

GD-enhancing tumor (ET), peritumoral edema (ED), and the necrotic and non-enhancing tumor core (NCR/NET). The study involved 369 subjects with 259 high-grade and 110 low-grade glioma, 125 validation cases, and 166 testing cases, with no publicly available segmentation masks. The samples of the database are presented in Figure 3.

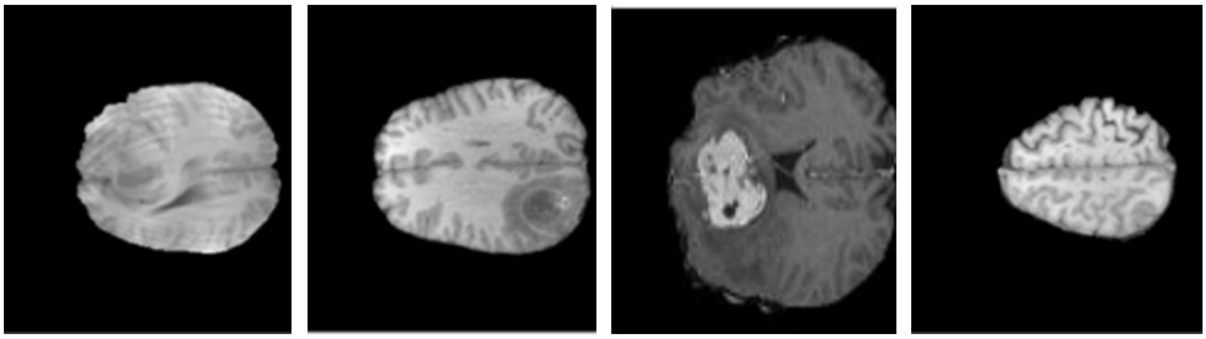

FIGURE 3. Sample dataset images

4.2. **Image preprocessing.** After data collection, the next step is image preprocessing. Image preprocessing defines the sequence of steps aimed at improving the image quality. The steps involved in image preprocessing include cropping, noise reduction, background elimination, and image resizing. The raw MRI images typically contain unwanted areas or regions, noises, backgrounds, etc., which may lead to poor image analysis and inaccurate tumor detection. Firstly, image cropping was done to remove the unwanted areas and regions from the images. This step involves adjusting the boundaries, selecting the region of interest (ROI), and pixel extraction to discard the unwanted regions. This enables the system to focus on the most relevant content, making the classification and further analysis more effective. Secondly, noise reduction was performed using the Gaussian filter while preserving the most important characteristics of the images. It reduces the noise features by convolving the input images with a Gaussian kernel, and it is mathematically represented in Equation **??**.

$$G_k(a,b) = I_m(a,b) * \frac{1}{2\pi\sigma^2} e^{-\frac{a^2+b^2}{2\sigma^2}} \tag{1}$$

Where $G_k(a, b)$ defines the filtered image, $I_m(a, b)$ denotes the input image, σ indicates the standard deviation of the Gaussian distribution, and (a, b) represents the kernel coordinates. This step not only eliminates the noise attributes but also smoothens the images. Further, thresholding was applied to eliminate the background from the images while restoring the useful content. Finally, bicubic interpolation was utilized to resize all images from the databases. After preprocessing, data augmentation steps, including flipping, rotation, shearing, scaling, and changing brightness, introduce diversity in the training sequence. These steps resolve the overfitting issues in the system training, improving the model's generalization.

4.3. **Image segmentation based on U-Net with EPO.** Image segmentation is defined as separating the preprocessed brain MRI images into different regions based on their characteristics in brain tumor classification. This plays a significant role in isolating the tumor region from healthy brain tissues. We developed an improved U-Net architecture for accurate and reliable tumor segmentation in the proposed work. The architecture of U-Net is classified into three components, namely: encoder, bottleneck, and decoder. The encoder accepts the preprocessed images as input, and the image's dimensions are 256×256. Typically, the encoder module utilizes convolution and pooling to downsample the images. In the improved U-Net, we use dense convolution instead of convolution. In the downsampling process, the size of the image was minimized while preserving the spatial attributes. Following downsampling operations, the images are fed into a deep neural network (DNN) for further processing. The DNN is the bottleneck component, which processes the feature maps obtained by the encoder part and extracts the high-level features from it. Finally, the images are forwarded into the decoder module, which utilizes upsampling algorithms to upscale the images. Here, deconvolution functions are applied to upscale images. The encoder and decoder components are interconnected with each other through skip connections. After a sequence of upsampling processes, the U-Net system produces segmented images with features. Further, we deploy the Emperor Penguin Optimizer (EPO) to optimize the weights and bias of the U-Net architecture. This valuable feature enables researchers to solve domain-specific problems by modifying EPO algorithm [30]. This optimization process aims to reduce cross-entropy loss, represented in Eqn. 2.

$$L_s(s, s') = -\sum_{i=1}^{n} s'(i) \log(s(i)) \tag{2}$$

Where $L_s(s, s')$ defines the loss function, n represents the number of classes, $s'(i)$ defines the probability of the i^{th} class in the ground truth, and $s(i)$ denotes the predicted probability of the i^{th} class generated by the model. The EPO is a meta-heuristic optimization algorithm, which was inspired and developed based on the social huddling characteristics of emperor penguins. The emperor penguins typically live in the Antarctic region, where the temperature falls very low during winter. This makes it very hard for the emperor penguins to survive, changing their characteristics to keep them warm. This process is called huddling and depends on numerous factors like distance, temperature, influential movers, etc. The proposed work applied EPO to minimize the loss by updating its weights during training. The EPO algorithm commences with the initialization of the emperor penguin population. In the proposed work, the emperor penguin population defines the population of candidate solutions (weights), which are randomly initialized. Then, the fitness value of each solution will be determined based on the predetermined objective function (cross-entropy loss). The fitness calculation is expressed in Eqn. (3).

$$f_w(t) = \frac{1}{L_s(s, s')} \tag{3}$$

The fitness value will be high if the loss incurred by the U-net for the candidate solution is low, and vice versa. After fitness evaluation, the values of each candidate solution are updated to find the optimal solution, which is mathematically expressed in Eqn. (4).

$$w(t+1) = w(t) - \vec{a} \cdot w^*(t) \tag{4}$$

Where $w(t+1)$ represents the updated candidate solution, $w(t)$ indicates the present value of the candidate solution, $w^*(t)$ denotes the best solution at iteration t, and $\vec{a}$ defines the factor preventing collision in exploration. After the exploration phase, the fitness value of the updated population was determined. If the updated fitness exceeds the old fitness, the updated weight will be used for U-Net training. This process is an iterative mechanism, making the system adaptable for diverse patient data and significantly improving the segmentation process.

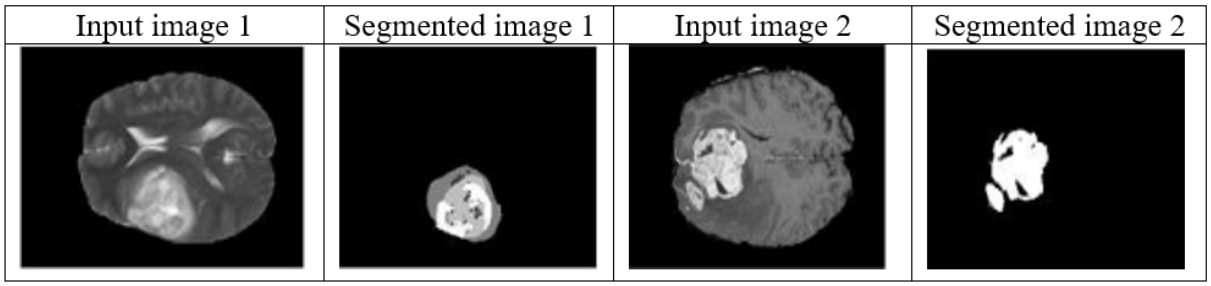

FIGURE 4. Input and segmented images

4.4. **Hybrid Feature Extraction based on FO with Transfer Learning (ResNet-50).** After image segmentation, the next step is feature extraction, which involves capturing and extracting the most informative and relevant attributes from the segmented images. This process aims to extract the characteristics of the segmented regions by quantifying their properties like shape, size, texture, intensity, etc., and these extracted feature sequences serve as input for the classifier for brain tumor classification tasks. We designed a hybrid feature extractor model in the proposed work by combining the optimization (FO) with the transfer learning algorithm (ResNet-50). The ResNet-50 is a pre-trained deep neural network capable of learning the high-level hierarchical representations of the segmented images. The ResNet-50 accepts segmented images as input and processes that extract the features. The segmented images are passed through five convolution layers to extract the feature sequence. Each convolution layer is designed with multiple residual blocks, and the residual block contains three convolutional layers. The first convolution layer contains 64 kernels, each having dimensions of [7x7x3]. This layer is followed by a maxpool layer with a filter size of [3x3]. Following this maxpool layer, four convolution layers are placed, each containing multiple residual blocks. The residual blocks contain three convolutional layers of dimensions [1x1], [3x3], and [1x1] with varying depths, progressively increasing from 64 to 2048. Following these convolutional layers, a maxpool layer is placed, followed by a fully connected layer with a size of 100. This fully connected layer acts as a feature extractor, producing the sequence of all features in the segmented images. This feature sequence was forwarded to the firefly optimization, which selects the most relevant and informative attributes for distinguishing the healthy and tumor classes. Firefly optimization (FO) is a nature-inspired optimization developed based

on the flashing characteristics of the fireflies. Firefly Algorithm (FA) is a highly efficient population-based optimization technique developed by mimicking the flashing behavior of fireflies when mating [31]. Like firefly initialization, we initialize the extracted feature sequence from the ResNet-50 block. The initialization of the feature set is represented in Eqn. (5).

$$f_{sq} = [f_1, f_2, f_3, \ldots, f_m] \tag{5}$$

Where f_{sq} indicates the extracted feature sequence and f_i defines the feature vector extracted from the image i. The primary objective of the FO block is to identify the features that differentiate the healthy and tumor classes. After initialization, the attractiveness between the features (f_i, f_j) is determined using the Eqn. (6).

$$A_{tr}(f_i, f_j) = e^{-\chi \|f_i - f_j\|^2} \tag{6}$$

Where χ defines the parameter controlling the strength of attractiveness. The attractiveness indicates the similarity between the features, enabling us to reduce the similar information from the extracted feature sequence. Also, it assists the system in exploring feature subsets containing diverse and complementary features. Following the attractiveness calculation, the feature vectors are updated and expressed in Eqn. (7).

$$f_i(t+1) = f_i(t) + \chi\, e^{-A_{tr}(f_i, f_j)}(f_i - f_j) + \alpha \tag{7}$$

Where t defines the iteration, α represents the randomness, and $f_i(t+1)$ denotes the updated feature. In this step, the feature vectors are updated based on their attractiveness to neighbor brighter solutions (features with a greater ability to differentiate normal and tumor classes). Then, the attractiveness was calculated for the updated feature subsets. Finally, the features with attractiveness of less than 0.5 are returned as the best solution (optimal features) and fed into the DCNN module for classifying tumors.

4.5. **Brain Tumor Classification Using DCNN.** A deep convolutional neural network is a kind of artificial neural network widely deployed in computer-vision tasks like image classification, objective detection, etc. In the developed work, we employed DCNN as a classifier model to categorize the healthy and tumor classes. The structure of DCNN is similar to that of CNN, with more than one convolutional layer. Using Deep CNN can greatly reduce the time and effort needed for feature engineering when it comes to picture classification [29]. Its general architecture includes five layers: an input layer, two or more convolutional layers, a pooling layer, a fully connected layer, and an output layer. The deep convolutional connections enable the system to learn hierarchical representations within the data, providing accurate classifications. The input layer accepts the extracted features as input. The convolutional layer uses kernel filters and captures the local patterns and correlations within the input sequence. As a result, it produces feature maps highlighting the spatial interconnections and patterns in the input data. The functioning of the convolutional layer is mathematically represented in Eqn. (8).

$$C_n = W_n * F_{se} + B_n \tag{8}$$

Where C_n defines the outcome of the n^{th} convolutional layer, W_n indicates the sequence of learnable parameters, F_{se} denotes the input features, and B_n represents the bias term of the n^{th} convolutional layer. The learnable parameters (filters) are adjusted in the training phase through backpropagation, which enables precise tumor classification. On the other hand, the pooling layers perform down sampling operations and reduce the spatial dimensions. This layer minimizes the feature dimensionality while preserving the

most significant attributes. Here, we applied max pooling to perform the above task. Finally, a fully connected layer was placed, which combined the learned patterns and corrections from the above layers to perform classifications. The output of the FC layer is defined in Eqn. (9).

$$F_c = A_f(W_f * P_o) + B_f \tag{9}$$

Where F_c represents the FC layer output, A_f defines the activation function, P_o denotes the learned patterns, W_f refers to the weight of the FC layer, and B_f indicates the bias term. The resultant of the FC layer is fed into the output layer, which is responsible for performing tumor classification. The output layer provides probability value based on the patterns and correlations learned, and it is presented in Eqn. (10).

$$P_s = softmax(W_o * F_c) + B_o \tag{10}$$

Where P_s defines the result of the output layer (probability value of classes), $softmax$ denotes the activation function, W_o indicates the weight of the output layer, and B_o refers to the output layer bias vector. The working of the proposed model is presented in pseudocode format in Algorithm 1.

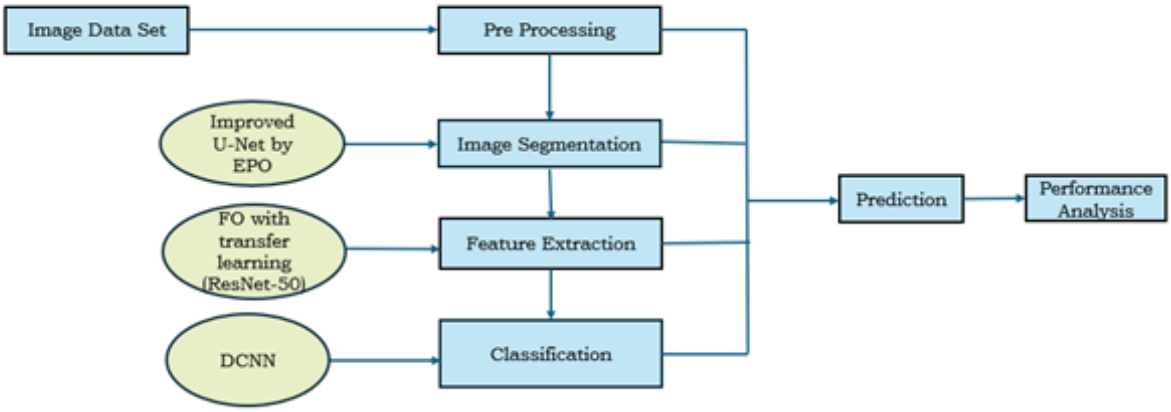

FIGURE 5. Flowchart of the proposed framework

5. **Experimental results and analysis.**

5.1. **Experimental environment and dataset.** In this study, we focused on developing improved image segmentation and feature extraction algorithms to classify brain tumors accurately. The presented framework was modeled on a Windows 11 Computer with an 11th-generation Intel Core i5 processor, 16 GB of RAM, and a 2GB graphics card. The Python language was used to model and implement the improved U-Net with EPO and feature extraction by FO with transfer learning (ResNet-50). The performances were assessed in terms of parameters such as accuracy, precision, recall, and f-measure.

5.2. **Performance evaluation.** In this section, we assess the training and testing performances of the proposed model. Firstly, we split the input database in the ratios 75:25 for model training and testing. In the training phase, the developed algorithm is trained using the training sequence to learn the data's patterns, features, and interconnections for differentiating healthy and tumor classes. On the other hand, testing defines the model

Algorithm 1 U-Net with EPO and Hybrid Feature Extraction (FO+ResNet-50)

Inputs: Brain MRI images; U-Net parameters; ResNet-50 parameters; DCNN parameters

Outputs: Classified tumor type (e.g., Meningioma, Glioma, Pituitary)

Image Preprocessing
Load brain MRI image dataset
for each image **do**
    Crop to region of interest (ROI)
    Apply Gaussian filter for noise reduction
    Eliminate background using thresholding or masking
    Resize image to 224×224
end for
Apply data augmentation (rotation, flipping, scaling, etc.)
Tumor Segmentation using Improved U-Net with EPO
Initialize U-Net architecture (encoder, bottleneck, decoder)
Initialize EPO parameters: population size, max iterations, initial solutions
for $t = 1$ **to** max_iterations **do**
    for each individual in population **do**
        Decode weights
        Apply U-Net forward pass
        Compute segmentation loss (e.g., Dice loss)
        Evaluate fitness = 1/loss
    end for
    Update weights using EPO behavior
    Retain weights with improved fitness
end for
Output segmented tumor region from trained U-Net
Feature Extraction using ResNet-50 and Firefly Optimization (FO)
Initialize pre-trained ResNet-50
for each segmented image **do**
    Feed image through ResNet-50
    Extract deep features from final pooling layers
end for
Initialize FO parameters: population of feature subsets, attractiveness threshold, iterations
for $t = 1$ **to** max_iterations **do**
    for each firefly **do**
        Calculate fitness based on feature subset performance
        Update position toward more attractive fireflies
        if attractiveness < 0.5 **then**
            Discard poor features
        end if
    end for
end for
Return optimized feature subset
Tumor Classification using DCNN
Initialize DCNN architecture
Train DCNN using optimized feature vectors from FO
Predict tumor class for each test image

Model Evaluation
Evaluate model using Accuracy, Precision, Recall, F1-score, and AUC/ROC
Return performance metrics and classified tumor labels

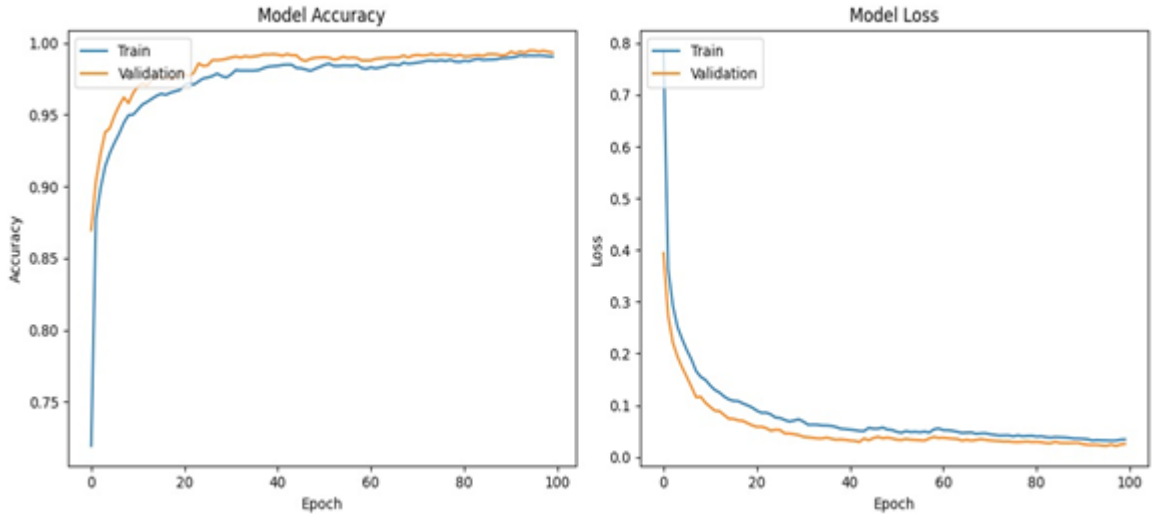

FIGURE 6. Model training and testing performances

evaluation over unseen brain MRI samples. This enables us to determine the model's generalization and how effectively it prevents the overfitting issue. The training and testing performances are assessed regarding accuracy and loss by increasing the number of epochs. The accuracy metric measures how well the developed algorithm learns the patterns and interconnections within the image samples and classifies the tumor instances. In contrast, the loss measures the deviation between the real and predicted outputs.

The training accuracy shows how well the proposed technique understands the pattern difference between the normal and tumor instances. The developed algorithm obtained higher training accuracy, demonstrating its faster learning capacity. Consequently, the testing or validation accuracy is evaluated, which determines the model's generalization over unknown MRI samples. The presented approach obtained greater testing accuracy over increasing epochs, highlighting that it generalizes well on the unseen data. Similar to accuracy, we determined loss in both the training and testing phases. The training loss depicts the difference between the real and predicted outcomes in the training sequence. The smaller training obtained by the developed model manifests that it fits the train set well, and it learns the hierarchical patterns and data representations more effectively. On the other hand, the testing loss determines the difference between the actual and the predicted results. It measures how the proposed technique resolves the overfitting challenge and accurately classifies the tumor classes.

The classification performance of the proposed model is presented in the confusion matrix. This table summarizes the proposed algorithm's classification performance by comparing the data's actual class labels with the class labels predicted by the technique. It utilizes four metrics for evaluating the model performances: true positive, true negative, false positive, and false negative. The true positive defines the number of instances correctly classified as positive (tumors), while the false positive represents the number of instances incorrectly categorized as positive. On the other hand, the true negative defines the number of instances that are correctly categorized as negative (healthy). In contrast, false negative represents the number of instances that are incorrectly classified as negative (tumor incorrectly predicted as normal).

Consequently, we analyzed the Receiver Operating Characteristics (ROC) curves. This curve represents the trade-off between a specific class's true and false positive rates. By analyzing the area under the curve (AUC), we also highlighted the model's capacity to differentiate each tumor class from others. The proposed model obtained an AUC greater

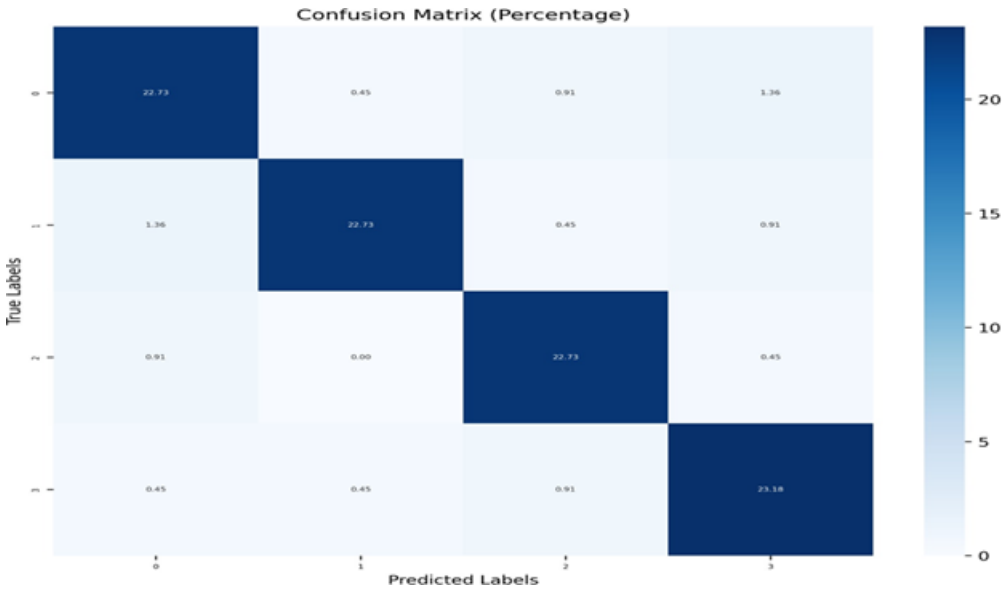

FIGURE 7. Confusion matrix

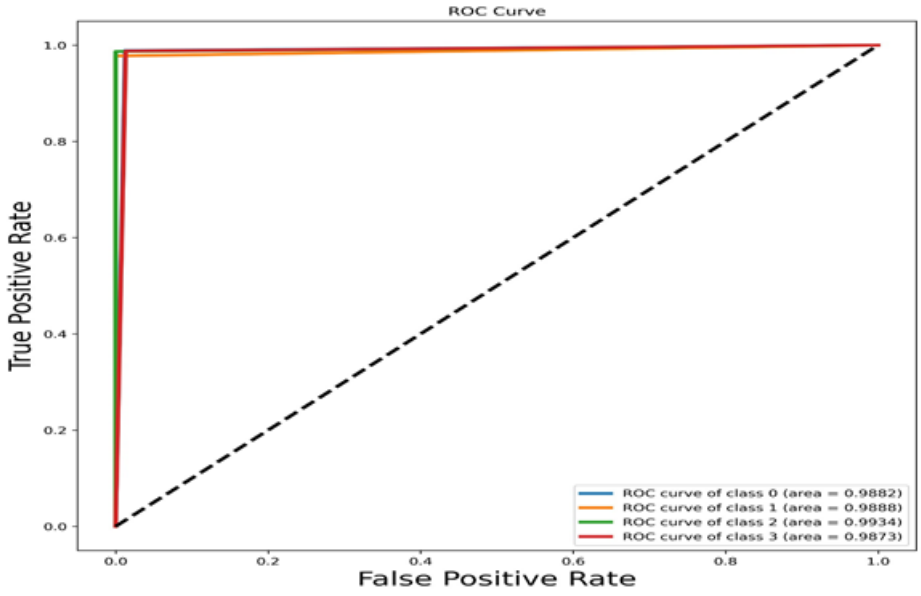

FIGURE 8. ROC curve

than 0.98, highlighting that it accurately classifies the tumor classes with a low false positive rate.

5.3. **Evaluation metrics.** In this section, we discuss the metrics used to evaluate the proposed model's performance. The performance metrics include classification accuracy, precision, recall, f-measure, Dice-similarity coefficient (DSC), and Jaccard Index (JI).

5.3.1. *Accuracy.* Accuracy defines the model's ability and correctness in detecting and classifying both healthy and tumor instances. It defines the ratio of true positive instances made by the model out of the total number of instances, and it is formulated in Eqn. (11).

$$Accuracy = \frac{T_{ps} + T_{nt}}{T_{ps} + T_{nt} + F_{ps} + F_{nt}} \tag{11}$$

Where T_{ps}, T_{nt}, F_{ps} and F_{nt} denote the true positive, true negative, false positive, and false negative, respectively.

5.3.2. *Precision.* Precision quantifies the accuracy of the positive predictions made by the classification model. It indicates the ratio of true positive predictions to the total number of positive predictions made by the system, and it is expressed mathematically in Eqn. (12).

$$Precision = \frac{T_{ps}}{T_{ps} + F_{ps}} \tag{12}$$

5.3.3. *Recall.* Recall quantifies the ratio of actual positive cases correctly detected and classified as positive by the proposed model. It is also known as sensitivity, and it is represented in Eqn. (13).

$$Recall = \frac{T_{ps}}{T_{ps} + F_{nt}} \tag{13}$$

5.3.4. *F-measure.* F-measure presents the harmonic mean of precision and recall metrics and offers a balanced evaluation of model performance considering both true and false instances. It is expressed in Eqn. (14).

$$F-measure = 2 \times \left(\frac{P_n \times R_a}{P_n + R_a} \right) \tag{14}$$

5.3.5. *Dice Similarity Coefficient (DSC).* DSC quantifies the overlap between the segmented and ground truth tumor regions. This metric evaluates the efficiency of the segmentation algorithm by measuring the similarity between the segmented and ground truth regions, and it is formulated in Eqn. (15).

$$DSC = \frac{2 \times |S \cap G|}{|S| + |G|} \tag{15}$$

Where S defines the segmented region and G denotes the ground truth tumor region.

5.3.6. *Jaccard Index (JI).* Jaccard Index, also defined as Intersection over Union (IoU), measures the similarity between the segmented and ground truth tumor regions. It is formulated in Eqn. (16).

$$JI = \frac{|S \cap G|}{|S \cup G|} \tag{16}$$

The evaluation of these metrics enables us to understand the proposed model's performance. Also, the assessment of DSC and JI enables us to determine the efficiency of the developed segmentation algorithm.

5.4. **Performance comparison.** In this section, we compare the performances of the proposed model with the existing techniques to validate its effectiveness and robustness in tumor classification. The existing methods used for comparative analysis include Enhanced Convolutional Neural Network (ECNN) [32], Hierarchical Deep Neural Network (HDNN) [33], Convolution Neural Network with Long Short-Term Memory (CNN-LSTM) [34], Whale Optimization-based Radial Neural Network (WO-RNN) [35], Social Spider Optimization with Radial Basis Neural Network (SSO-RBNN) [36], and Fully Optimized Convolutional Neural Network (FOCNN) [37]. The performances of these

techniques are determined by implementing them on the Python tool for the same input database, and outcomes are determined in terms of accuracy, precision, recall, and f-measure.

The accuracy metrics measure how well the developed model learns the patterns and interconnections between the healthy and the tumor instances. Figure **??** presents the comparison of accuracy. The existing techniques, such as ECNN, HDNN, CNN-LSTM, WO-RNN, SSO-RBNN, and FOCNN, obtained an accuracy of 94.62%, 90.10%, 96.17%, 95.30%, 92.65%, and 94.36%, respectively, while the proposed approach obtained higher accuracy of 99.80%. This improved accuracy depicts that the utilization of enhanced image segmentation and feature extraction algorithms increases the model's classification accuracy.

Consequently, the precision performance of the developed technique was validated with the existing methods, and it is graphically presented in Figure **??**. The conventional approaches, such as ECNN, HDNN, CNN-LSTM, WO-RNN, SSO-RBNN, and FOCNN, achieved precision of 94.18%, 89.17%, 95.68%, 95.58%, 91.37%, and 94.48%, respectively. On the other hand, the proposed technique obtained an improved precision of 99.44%, highlighting that it more accurately predicts tumor instances than the conventional models.

The recall metric measures the model's ability to classify actual tumor instances as positive. It also defines the model's ability to extract all relevant attributes for differentiating the healthy and tumor instances. Figure **??** presents the comparison of recall with existing techniques. The existing techniques, including ECNN, HDNN, CNN-LSTM, WO-RNN, SSO-RBNN, and FOCNN, attained recall of 94.34%, 89.58%, 96.22%, 94.62%, 92.50%, and 94.10%, respectively, while the designed approach achieved greater recall rate of 99.55%.

Finally, the F-measure performance of the developed algorithm is validated with the conventional models, which is presented in Figure **??**. The above-stated existing techniques obtained f-measures of 94.37%, 89.48%, 95.06%, 94.81%, 92.33%, and 94.05%, respectively, while the developed algorithm obtained higher f-measures of 99.49%. The improved f-measures highlight the model's capacity to accurately identify the tumor and healthy images. Table 2 presents the comparative analysis of classification performances.

Table 2. Comparative Performance Analysis

Methods	**Accuracy (%)**	**Precision (%)**	**Recall (%)**	**F-measure (%)**
ECNN	94.62	94.18	94.34	94.37
HDNN	90.10	89.17	89.58	89.48
CNN-LSTM	96.17	95.68	96.22	95.06
WO-RNN	95.30	95.58	94.62	94.81
SSO-RBNN	92.65	91.37	92.50	92.33
FOCNN	94.36	94.48	94.10	94.05
Proposed	**99.80**	**99.44**	**99.55**	**99.49**

5.5. **Comparison of Segmentation Algorithm Performances.** In this subsection, we compare and evaluate the segmentation efficiency of the developed improved U-Net algorithm with the existing segmentation techniques like U-Net, ResNet, VGG-16, VGG-19, and DenseNet. The parameters used for comparative analysis include DSC and JI.

The DSC measures the segmentation accuracy of the models by measuring the similarity between the segmented and the actual ground truth tumor regions. Here, we compare the DSC performance of the improved U-Net architecture with conventional algorithms

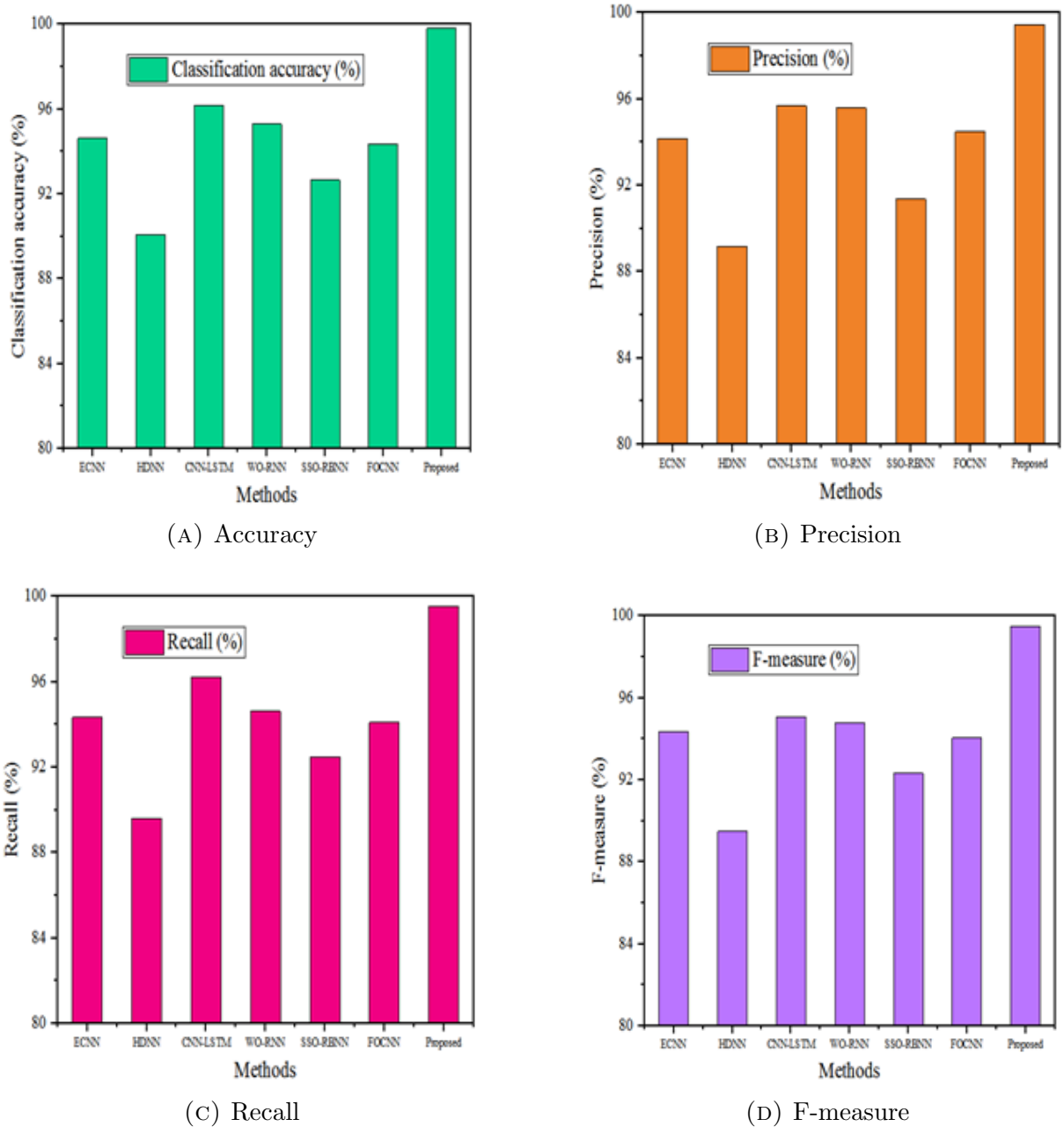

(A) Accuracy (B) Precision

(C) Recall (D) F-measure

FIGURE 9. Comparative Analysis of Proposed Model with Existing Methods

like U-Net, ResNet, VGG-16, VGG-19, and DenseNet. These models obtained DSCs of 0.98, 0.97, 0.96, 0.97, and 0.95, respectively, while the proposed approach obtained a higher DSC of 0.995. The improved DSC defines that the proposed improved U-Net architecture offers more accurate segmentation of tumor regions than the conventional models. Figure 10 (a, b) compares DSC and JI performances.

Consequently, we validated the developed model's JI performance with the existing techniques. The existing methods, such as U-Net, ResNet, VGG-16, VGG-19, and DenseNet, obtained JI performance of 0.982, 0.973, 0.956, 0.962, and 0.967, respectively, while the developed improved U-Net algorithm achieved a higher JI performance of 0.996. The enhanced JI performance highlights the model's capacity to segment the tumor regions correctly.

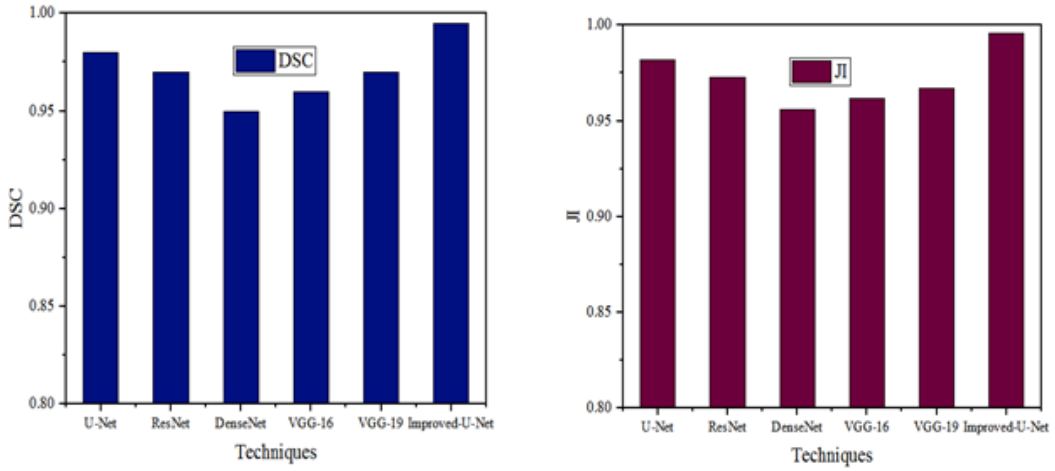

(A) DSC (B) JI

FIGURE 10. Comparative Analysis of Segmentation Performances

TABLE 3. Comparative Performance Of Segmentation Algorithms

Techniques	DSC	JI
U-Net	0.98	0.982
ResNet	0.97	0.973
DenseNet	0.95	0.956
VGG-16	0.96	0.962
VGG-19	0.97	0.967
Improved-U-Net	0.995	0.996

The comparison of DSC and JI performances is tabulated in Table 3. The proposed improved U-Net algorithm obtained higher DSC and JI performances than the conventional models, highlighting its efficiency in segmenting the tumor regions as accurately as ground truth tumor regions.

6. **Discussion.** The proposed model combines an improved U-Net with Emperor Penguin Optimization (EPO), ResNet-50 for deep feature extraction, and Firefly Optimization (FO) for feature selection. High classification performance, efficient feature extraction, and precise segmentation are the main issues in brain tumor identification with MRI images that the system is designed to overcome.

6.1. **Analysis of Results.** The experimental results demonstrate segmentation and classification metrics compared to existing methods. The proposed model achieved a classification accuracy of 99.80%, precision of 99.44%, recall of 99.55%, and F1-score of 99.49%, while the segmentation performance attained a Dice Similarity Coefficient (DSC) of 0.995 and Jaccard Index (JI) of 0.996. These results underscore the model's capability in accurately segmenting and classifying brain tumors from MRI scans.

Several factors contributed to this performance:

- Accurate Segmentation with EPO-U-Net: The incorporation of Emperor Penguin Optimization into the U-Net training phase enables more precise weight optimization. Unlike conventional gradient-based methods, EPO enhances convergence and avoids local minima, resulting in better tumor boundary detection.

- Deep Feature Representation using ResNet-50: ResNet-50 successfully captures complex texture and structural patterns from segmented images. Its residual blocks allow for deeper architectures without vanishing gradients, enabling robust feature extraction.
- Feature Selection via Firefly Optimization: The FO algorithm discards redundant or irrelevant features, improving classification speed and accuracy. This selective process contributes to reduced overfitting, especially on smaller datasets.
- End-to-End Pipeline Efficiency: By combining segmentation, deep feature extraction, and classification into a seamless pipeline, the model reduces manual preprocessing steps and supports automation.

The proposed method offers several advantages, including high accuracy in classification and segmentation, improved learning through optimization techniques, robustness against noise and variability, and enhanced feature discriminability enabled by deep transfer learning combined with metaheuristic algorithms.

6.2. **Limitations and Challenges.**

- Computational Cost: The inclusion of metaheuristic optimizations (EPO and FO) increases computational time and resource requirements, especially during training.
- Hyperparameter Sensitivity: The performance of EPO and FO depends heavily on parameters like population size, iterations, and attraction coefficients, which require careful tuning.
- Generalization on External Datasets: Although results are strong on the tested dataset, further validation is needed on external, diverse datasets to confirm generalizability.
- Explainability Concerns: Deep learning and metaheuristics lack interpretability, which may hinder clinical trust and adoption.

7. **Conclusion.**

This study developed an improved segmentation and hybrid feature extraction algorithm for accurately classifying brain tumors using MRI images. The study's novelty lies in the seamless integration of optimization and transfer learning models for accurate segmentation and effective feature extraction. Firstly, the images are collected from the site and preprocessed to improve their quality and make them effective for further analysis. Then, we performed tumor segmentation using the proposed improved U-Net architecture. Consequently, feature extraction was done using the developed hybrid FO-ResNet-50 model, which enables the capture and extraction of the most informative and discriminative features for tumor classification. Finally, we trained the DCNN model with the extracted features to distinguish healthy and tumor classes. The proposed study was trained and validated using the BraTS 2020 database. The experimental results depict that the developed model achieved a high classification accuracy of 99.80%, improved precision of 99.44%, greater recall of 99.55%, and enhanced f-measure of 99.49%. In addition, the developed segmentation algorithm achieved a greater DSC of 0.995 and JI of 0.996, highlighting its efficiency in segmenting the tumor regions more effectively. Finally, we made a comparative assessment with the existing techniques, and it validated that the developed algorithm outperformed the existing models. These improved performances of the proposed approach make it effective and reliable for real-time brain tumor segmentation and classification. Future research will focus on incorporating explainable AI, reducing complexity through model compression and lightweight architectures, expanding validation using multicentre and cross-domain datasets, and exploring other metaheuristic algorithms or hybrid optimization techniques.

REFERENCES

[1] Milstein, Joshua L., and Heather A. Ferris. "The brain as an insulin-sensitive metabolic organ." *Molecular Metabolism*, vol. 52, 2021, 101234.

[2] Amin, Javaria, et al. "Brain tumor detection and classification using machine learning: a comprehensive survey." *Complex & Intelligent Systems*, vol. 8, no. 4, 2022, pp. 3161–3183.

[3] Gavas, Shreelaxmi, Sameer Quazi, and Tomasz M. Karpiński. "Nanoparticles for cancer therapy: current progress and challenges." *Nanoscale Research Letters*, vol. 16, no. 1, 2021, 173.

[4] Zhu, Yingze, et al. "Small-cell lung cancer brain metastasis: From molecular mechanisms to diagnosis and treatment." *Biochimica et Biophysica Acta (BBA)-Molecular Basis of Disease*, vol. 1868, no. 12, 2022, 166557.

[5] Rizwan, Muhammad, et al. "Brain tumor and glioma grade classification using Gaussian convolutional neural network." *IEEE Access*, vol. 10, 2022, pp. 29731–29740.

[6] Pettersson-Segerlind, Jenny, et al. "Long-term follow-up, treatment strategies, functional outcome, and health-related quality of life after surgery for WHO grade 2 and 3 intracranial meningiomas." *Cancers*, vol. 14, no. 20, 2022, 5038.

[7] Salari, Nader, et al. "The global prevalence of primary central nervous system tumors: a systematic review and meta-analysis." *European Journal of Medical Research*, vol. 28, no. 1, 2023, 39.

[8] Van Damme, Julien, et al. "Comparison of 68Ga-prostate specific membrane antigen (PSMA) positron emission tomography computed tomography (PET-CT) and whole-body magnetic resonance imaging (WB-MRI) with diffusion sequences (DWI) in the staging of advanced prostate cancer." *Cancers*, vol. 13, no. 21, 2021, 5286.

[9] Nawaz, Marriam, et al. "Analysis of brain MRI images using improved cornernet approach." *Diagnostics*, vol. 11, no. 10, 2021, 1856.

[10] Abdou, Mohamed A. "Literature review: Efficient deep neural networks techniques for medical image analysis." *Neural Computing and Applications*, vol. 34, no. 8, 2022, pp. 5791–5812.

[11] Huang, Qinghua, et al. "A novel image-to-knowledge inference approach for automatically diagnosing tumors." *Expert Systems with Applications*, vol. 229, 2023, 120450.

[12] Budati, Anil Kumar, and Rajesh Babu Katta. "An automated brain tumor detection and classification from MRI images using machine learning techniques with IoT." *Environment, Development and Sustainability*, vol. 24, no. 9, 2022, pp. 10570–10584.

[13] Barragán-Montero, Ana, et al. "Artificial intelligence and machine learning for medical imaging: A technology review." *Physica Medica*, vol. 83, 2021, pp. 242–256.

[14] Soori, Mohsen, Behrooz Arezoo, and Roza Dastres. "Artificial intelligence, machine learning and deep learning in advanced robotics, a review." *Cognitive Robotics*, vol. 3, 2023, pp. 54–70.

[15] Houssein, Essam H., et al. "Deep and machine learning techniques for medical imaging-based breast cancer: A comprehensive review." *Expert Systems with Applications*, vol. 167, 2021, 114161.

[16] Ngugi, Lawrence C., Moataz Abelwahab, and Mohammed Abo-Zahhad. "Recent advances in image processing techniques for automated leaf pest and disease recognition – A review." *Information Processing in Agriculture*, vol. 8, no. 1, 2021, pp. 27–51.

[17] García, Gabriel, et al. "A novel self-learning framework for bladder cancer grading using histopathological images." *Computers in Biology and Medicine*, vol. 138, 2021, 104932.

[18] Cruz-Ramos, Clara, et al. "Benign and malignant breast tumor classification in ultrasound and mammography images via fusion of deep learning and handcraft features." *Entropy*, vol. 25, no. 7, 2023, 991.

[19] Shamshirband, Shahab, et al. "A review on deep learning approaches in healthcare systems: Taxonomies, challenges, and open issues." *Journal of Biomedical Informatics*, vol. 113, 2021, 103627.

[20] Painuli, Deepak, and Suyash Bhardwaj. "Recent advancement in cancer diagnosis using machine learning and deep learning techniques: A comprehensive review." *Computers in Biology and Medicine*, vol. 146, 2022, 105580.

[21] Sharif, Muhammad Imran, et al. "A decision support system for multimodal brain tumor classification using deep learning." *Complex & Intelligent Systems*, 2021, pp. 1–14.

[22] Ghassemi, Navid, Afshin Shoeibi, and Modjtaba Rouhani. "Deep neural network with generative adversarial networks pre-training for brain tumor classification based on MR images." *Biomedical Signal Processing and Control*, vol. 57, 2020, 101678.

[23] Kang, Jaeyong, Zahid Ullah, and Jeonghwan Gwak. "MRI-based brain tumor classification using ensemble of deep features and machine learning classifiers." *Sensors*, vol. 21, no. 6, 2021, 2222.

[24] Raza, Asaf, et al. "A hybrid deep learning-based approach for brain tumor classification." *Electronics*, vol. 11, no. 7, 2022, 1146.
[25] Kuraparthi, Swaraja, et al. "Brain Tumor Classification of MRI Images Using Deep Convolutional Neural Network." *Traitement du Signal*, vol. 38, no. 4, 2021.
[26] Gull, Sahar, and Shahzad Akbar. "Artificial intelligence in brain tumor detection through MRI scans: advancements and challenges." *Artificial Intelligence and Internet of Things*, 2021, pp. 241–276.
[27] Jena, Biswajit, et al. "Analysis of depth variation of U-NET architecture for brain tumor segmentation." *Multimedia Tools and Applications*, vol. 82, no. 7, 2023, pp. 10723–10743.
[28] Anand, R., et al. "An enhanced ResNet-50 deep learning model for arrhythmia detection using electrocardiogram biomedical indicators." *Evolving Systems*, vol. 15, no. 1, 2024, pp. 83–97.
[29] Towfek, S. K., and Nima Khodadadi. "Deep convolutional neural network and metaheuristic optimization for disease detection in plant leaves." *Journal of Intelligent Systems and Internet of Things*, vol. 10, no. 1, 2023, pp. 66–75.
[30] Khalid, Othman Waleed, Nor Ashidi Mat Isa, and Harsa Amylia Mat Sakim. "Emperor penguin optimizer: A comprehensive review based on state-of-the-art meta-heuristic algorithms." *Alexandria Engineering Journal*, vol. 63, 2023, pp. 487–526.
[31] Zare, Mohsen, et al. "A global best-guided firefly algorithm for engineering problems." *Journal of Bionic Engineering*, vol. 20, no. 5, 2023, pp. 2359–2388.
[32] Singh, Ravendra, and Bharat Bhushan Agarwal. "An automated brain tumor classification in MR images using an enhanced convolutional neural network." *International Journal of Information Technology*, vol. 15, no. 2, 2023, pp. 665–674.
[33] Shajin, Francis H., et al. "Efficient framework for brain tumour classification using hierarchical deep learning neural network classifier." *Computer Methods in Biomechanics and Biomedical Engineering: Imaging & Visualization*, vol. 11, no. 3, 2023, pp. 750–757.
[34] Vankdothu, Ramdas, Mohd Abdul Hameed, and Husnah Fatima. "A brain tumor identification and classification using deep learning based on CNN-LSTM method." *Computers and Electrical Engineering*, vol. 101, 2022, 107960.
[35] Dixit, Asmita, and Aparajita Nanda. "An improved whale optimization algorithm-based radial neural network for multi-grade brain tumor classification." *The Visual Computer*, vol. 38, no. 11, 2022, pp. 3525–3540.
[36] Nanda, Aparajita, Ram Chandra Barik, and Sambit Bakshi. "SSO-RBNN driven brain tumor classification with Saliency-K-means segmentation technique." *Biomedical Signal Processing and Control*, vol. 81, 2023, 104356.
[37] Irmak, Emrah. "Multi-classification of brain tumor MRI images using deep convolutional neural network with fully optimized framework." *Iranian Journal of Science and Technology, Transactions of Electrical Engineering*, vol. 45, no. 3, 2021, pp. 1015–1036.
[38] Qureshi, Shahzad Ahmad, et al. "RobU-Net: A heuristic robust multi-class brain tumor segmentation approaches for MRI scans." *Waves in Random and Complex Media*, 2024, pp. 1–51.
[39] Qureshi, Shahzad Ahmad, et al. "Radiogenomic classification for MGMT promoter methylation status using multi-omics fused feature space for least invasive diagnosis through mpMRI scans." *Scientific Reports*, vol. 13, no. 1, 2023, 3291.
[40] Amudha, P. "Enhanced Brain Tumor Detection via Multiscale Frangi Gaussian Matrix and Efficient Convolutional Networks on MRI." 2024.
[41] Mohammad Anwar Assaad, Maral Ismael Saleh, and Rania Mahrousseh. "A Novel Framework for Accurate Brain Tumor Detection in MRI Scans Using CNN, MLP, and KNN Techniques." *Journal of Information Hiding and Multimedia Signal Processing*, vol. 16, no. 2, pp. 590–602, June 2025.